UCRL-JRNL-231148

LAWRENCE
LIVERMORE
NATIONAL
LABORATORY

Particle Simulation of Coulomb Collisions: Comparing the Methods of Takizuka & Abe and Nanbu

C. Wang, T. Lin, R. Caflisch, B. Cohen, A. Dimits

May 23, 2007

Disclaimer

This document was prepared as an account of work sponsored by an agency of the United States Government. Neither the United States Government nor the University of California nor any of their employees, makes any warranty, express or implied, or assumes any legal liability or responsibility for the accuracy, completeness, or usefulness of any information, apparatus, product, or process disclosed, or represents that its use would not infringe privately owned rights. Reference herein to any specific commercial product, process, or service by trade name, trademark, manufacturer, or otherwise, does not necessarily constitute or imply its endorsement, recommendation, or favoring by the United States Government or the University of California. The views and opinions of authors expressed herein do not necessarily state or reflect those of the United States Government or the University of California, and shall not be used for advertising or product endorsement purposes.

Particle Simulation of Coulomb Collisions: Comparing the methods of Takizuka & Abe and Nanbu

Chiaming Wang, Tungyou Lin, and Russel Caflisch

Mathematics Department, University of California at Los Angeles, Los Angeles, CA 90036 USA

Bruce Cohen and Andris Dimits

Lawrence Livermore National Laboratory, Livermore CA 94550 USA

The interactions of charged particles in a plasma are in a plasma is governed by the long-range Coulomb collision. We compare two widely used Monte Carlo models for Coulomb collisions. One was developed by Takizuka and Abe in 1977, the other was developed by Nanbu in 1997. We perform deterministic and stochastic error analysis with respect to particle number and time step. The two models produce similar stochastic errors, but Nanbu's model gives smaller time step errors. Error comparisons between these two methods are presented.

I. INTRODUCTION

A plasma consists of a large number of charged particles. An appropriate method to describe a plasma state is a statistical approach, *i.e.* a distribution function provides a complete description of the system. If a plasma is highly collisional, its distribution function will be rapidly driven to thermodynamical equilibrium, and the plasma kinetics can be approximated by a fluid description. On the other hand, if a plasma is collisionless, the plasma is not in equilibrium, and each particle interacts with the rest of the plasma through collective effects of long-range electromagnetic fields. In the intermediate regime between the two cases, collisional effects have to be included specifically to provide an adequate description of plasma kinetics. One significant example is the edge plasmas (scrape-off layer) in a confinement fusion device. A fluid approximation is not valid since the high energy (superthermal) electrons result in a relatively large ratio of mean free path to the system's characteristic length. A kinetic approach is essential for satisfactory physical modeling and numerical simulations for such plasmas [1].

One feature which distinguishes a plasma from a fluid is that its particles are charged

and have long-range Coulomb interactions. A particle in a plasma has distance encounters with many other particles simultaneously, and each encounter produces a small collisional effect on the particle. The scattering of particles due to multiple small collisions is dominant and is more important than the single large-angle scattering. For this reason, the Coulomb scattering angle can be treated as the cumulative deflection of a series of small angle binary collisions [2].

One of the earliest and most influential Monte Carlo binary collision models was proposed by T. Takizuka & H. Abe in 1977 [3]. In their method, the domain is divided into cells and particles are grouped within each cell. Randomly chosen pairs of particles undergo binary collisions. The resulting scattering angle is sampled through a Gaussian distribution to compute the change in velocities. Their method simulates each small angle collision and requires a time step much smaller than the overall relaxation time for the entire velocity distribution function.

Nanbu proposed a new Monte Carlo binary collision model in 1997 [4]. His method uses the idea that a Coulomb collision can be described by many continuous small angle binary collisions [2]. Nanbu's method computes the cumulative scattering angle for many small binary deflections. Successive small angles are grouped into one single collision angle. This suggests that a larger time step may be used in his method.

The two methods proposed by Takizuka & Abe and Nanbu have been widely used in the plasma physics community. Nanbu's method has been considered more efficient than Takizuka & Abe's method because it computes an accumulative Coulomb scattering angle rather than a single Coulomb scattering angle one by one. For this reason, we are interested in performing convergence analysis to compute the errors and to derive the orders of accuracy for both methods to quantitatively compare their performance and relative efficiencies. We also believe their models have potential to be used to extend the hybrid method for rarefied gas [5] to plasma with Coulomb collisions.

For simplicity, in this article we call the collision model developed by Takizuka and Abe "TA's method" and the model developed by Nanbu "Nanbu's method". To test these two models, we use a test problem that consists of a spatially homogeneous plasma with no electric or magnetic fields, as described in [3], [4]. We simulate the relaxation of anisotropic Maxwellian distribution (i.e. a distriubtion with anisotropic temperatures) over time due to collisions, using the results to evaluate the accuracy and efficiency of these two methods. We

test both electron-electron and electron-ion collision cases and obtain comprehensive convergence results. We find a few similarities of the results computed using the two methods. For the average solutions, both methods have square root time step accuracy $O(\sqrt{\Delta t})$. The random errors are independent of time step, and diminish like $O(N^{-\frac{1}{2}})$ when the number of particles N grows. In the conclusion, we evaluate the significance of the results, as well as consider some advantages to Nanbu's method and its possible applications.

The article is organized as follows. First we describe the collision models formulated by Takizuka & Abe, and Nanbu in section 2. In section 3, we propose a test case and define the quantities for the convergence analysis. Next, we present the simulation results for Nanbu's method and TA's method, and compare the differences in the results obtained in section 4. Concluding remarks and a summary are offered in section 5.

II. GENERAL FORMULATION

We first introduce the governing equation for the physical process, and describe TA and Nanbu's Monte Carlo binary collision models. We will emphasize the major distinguishing aspect of the two collision models: computing the scattering angle of two colliding particles. We consider collisions between N particles from two species alpha and beta. For simplicity, we assume that N is even. If alpha and beta are different, we also assume that there are $N/2$ α particles and $N/2$ β particles.

A. Governing equation

The time evolution of the particle distribution in a non-equilibrium plasma is described by the Fokker Planck equation:

$$\frac{\partial f_\alpha}{\partial t} + \mathbf{v} \cdot \nabla_x f_\alpha + \frac{e}{m}(E + \mathbf{v} \times B) \cdot \nabla_v f_\alpha = (\frac{\delta f_\alpha}{\delta t})_c$$

$$f_\alpha(\mathbf{v}, \mathbf{x}, 0) = f_{\alpha 0}(\mathbf{v}, \mathbf{x})$$

where f_α is the distribution function of the α species, E is the electric field, and B is the magnetic field. $(\frac{\delta f}{\delta t})_c$ is the collision operator and defined as the following:

$$(\frac{\delta f_\alpha}{\delta t})_c = -\sum_\beta \frac{\partial}{\partial v_j} \frac{e_\alpha^2 e_\beta^2 \lambda}{8\pi\epsilon_0^2 m_\alpha} \int dv' [\frac{\delta_{jk}}{u} - \frac{u_j u_k}{u^3}][\frac{f_\alpha}{m_\beta} \frac{\partial f_\beta(v')}{\partial v_k'} - \frac{f_\beta'}{m_\alpha} \frac{\partial f_\alpha}{\partial v_k}]. \tag{1}$$

The equation for f_β is similar.

TA and Nanbu's collision models can be considered as numerical approximations to the Fokker Planck collision operator. We will discuss the two models for a spatially homogeneous plasma in the following two sections.

B. Takizuka and Abe's Collision Model

The scattering angle in TA's method is defined in the relative velocity frame. First two particles with velocity v_α and v_β are selected. Let Θ be the scattering angle between two particles in the relative frame. The angle Θ is sampled randomly through a random variable δ related to Θ by the function tan. Specifically,

$$\delta \equiv \tan(\Theta/2) \tag{2}$$

where δ is a Gaussian random variable which has mean 0 and the following variance

$$< \delta^2 > = (\frac{e_\alpha^2 e_\beta^2 n_L \log \Lambda}{8\pi \epsilon_0^2 m_{\alpha\beta}^2 u^3})\Delta t$$

where e_α and e_β are electric charges for the species α and β, n_L is the smaller density of the particle species α and β, Λ is the Coulomb logarithm, $u = |v_\alpha - v_\beta|$ is the relative speed, Δt is the time step , and $m_{\alpha\beta}$ is the reduced mass and is defined as follows:

$$m_{\alpha\beta} = \frac{m_\alpha m_\beta}{m_\alpha + m_\beta}.$$

To compute the velocity changes of the particles due to collision, a Gaussian random variable δ is sampled and used to compute $\sin\Theta$ and $\cos\Theta$ through the following formulas derived from (2):

$$\sin\Theta = \frac{2\delta}{(1 + \delta^2)}$$
$$1 - \cos\Theta = 2\delta^2/(1 + \delta^2).$$

$\sin\Theta$ and $\cos\Theta$ are then used to compute the postcollisional velocities v_α', v_β' of the two particles [3].

$$v_\alpha' = v_\alpha + \frac{m_{\alpha\beta}}{m_\alpha}\Delta u$$

4

$$v'_\beta = v_\beta - \frac{m_{\alpha\beta}}{m_\beta}\Delta u$$

and Δu is defined as follows:

$$u = v_\alpha - v_\beta,$$

$$\Delta u_x = (u_x/u_\perp)u_z \sin\Theta \cos\Phi - (u_y/u_\perp)u \sin\Theta \sin\Phi - u_x(1 - \cos\Theta),$$

$$\Delta u_y = (u_y/u_\perp)u_z \sin\Theta \cos\Phi + (u_x/u_\perp)u \sin\Theta \sin\Phi - u_y(1 - \cos\Theta),$$

$$\Delta u_z = -u_\perp \sin\Theta \cos\Phi - u_z(1 - \cos\Theta),$$

and $u_\perp = \sqrt{u_x^2 + u_y^2}$. The azimuthal angle Φ is randomly chosen from on the uniform interval $[0, 2\pi]$.

In each time step, TA's method groups all of the N particles into N/2 pairs, each consisting of an alpha particle and a beta particle, and performs a single collision for each pair. The random selection of partcle pairs through many time steps approximates the integration of the distribution function over the particles. The method's cross section represents the Fokker-Planck process. Hence, TA's method directly simulates the Fokker-Planck collision operator (1).

C. Nanbu's Collision Model

Coulomb collisions in a plasma can be treated as the simulation of many continuous small angle binary collisions [2]. Rather than computing every small angle binary collisions as in TA's method, Nanbu's method provides a procedure to compute the aggregated scattering angle of many small angle binary collisions for a given pair of velocities v_α and v_β.

Let $\mathbf{g_0}$ be the initial velocity and $\mathbf{g_1}, \mathbf{g_2}, ..., \mathbf{g}_N$ be the postcollision velocities after first, second,..., and N collisions. Let χ_N be the cumulative scattering angle after N collisions. χ_N is defined as the following

$$\cos\chi_N = \mathbf{g_0} \cdot \mathbf{g_N}/g^2$$

where $g = |\mathbf{g_0}|$. χ_N can be obtained through the following three steps:

1. At the beginning of the time step, calculate a quantity s

$$s = n_\beta g\pi b_0^2(\ln\Lambda)\Delta t$$

   where b_0 is the impact parameter, n_β is the density of field particles, Λ is the Coulomb logarithm and Δt is the time step.

5

2. Use s to determine a constant A from the following equation:

$$\coth A - A^{-1} = e^{-s}$$

The constant A will be used to define the probability density of χ_N.

3. Sam;ple cumulative scattering angle χ_N with the following probability density function $F(\chi_N)$:

$$F(\chi_N) = \frac{2\pi A}{4\pi \sin hA} e^{A\cos\chi} \sin\chi_N.$$

The velocities after cumulative collisions are

$$\mathbf{v}'_\alpha = \mathbf{v}_\alpha - \frac{m_{\alpha\beta}}{m_\alpha}[\mathbf{g}(1-\cos\chi) + \mathbf{h}\sin\chi],$$

$$\mathbf{v}'_\beta = \mathbf{v}_\beta + \frac{m_{\alpha\beta}}{m_\beta}[\mathbf{g}(1-\cos\chi) + \mathbf{h}\sin\chi],$$

where $\mathbf{g} = \mathbf{v}_\alpha - \mathbf{v}_\beta$ and $\mathbf{h} = (h_x, h_y, h_z)$ with

$$h_x = g_\perp \cos\epsilon,$$

$$h_y = -(g_y g_x \cos\epsilon + g g_z \sin\epsilon)/g_\perp$$

$$h_z = -(g_z g_x \cos\epsilon - g g_y \sin\epsilon)/g_\perp$$

and $g_\perp = \sqrt{g_x^2 + g_y^2}$ and ϵ is a random number uniformly distributed in $[0, 2\pi]$.

Nanbu's method is motivated by physical considerations associated with Coulomb collisions in the Fokker-Planck limit. In a subsequent work, Bobylev and Nanbu [6] derive a time-explicit formula to approximate the time evolution of plasmas from the Boltzmann equation. Their analysis theoretically verifies that, when $\Delta t \to 0$, the numerical solutions computed using Nanbu's method are the solutions of the Fokker-Planck equation. More specifically, the method approximates the collision operator J of the Boltzmann equation by an exponential operator defined by J and then solves an initial value problem using spherical harmonic functions to define the time evolution formula. Similar to the idea that is used to derive Fokker-Planck equation from the Boltzmann equation [7], small-angle scattering leads to the formula for computing the evolution of a velocity distribution:

$$f_\alpha(\mathbf{v}, t+\Delta t) = \sum_{\beta=1}^{n} \pi_{\alpha\beta} \int_{R^3 \times S^2} d\mathbf{w} d\mathbf{n} D_{\alpha\beta}(\frac{\mathbf{g}\cdot\mathbf{n}}{g}, \Lambda\frac{\Delta t}{g^3}) f_\alpha(\mathbf{v}'_\alpha, t) f_\beta(\mathbf{v}'_\beta, t).$$
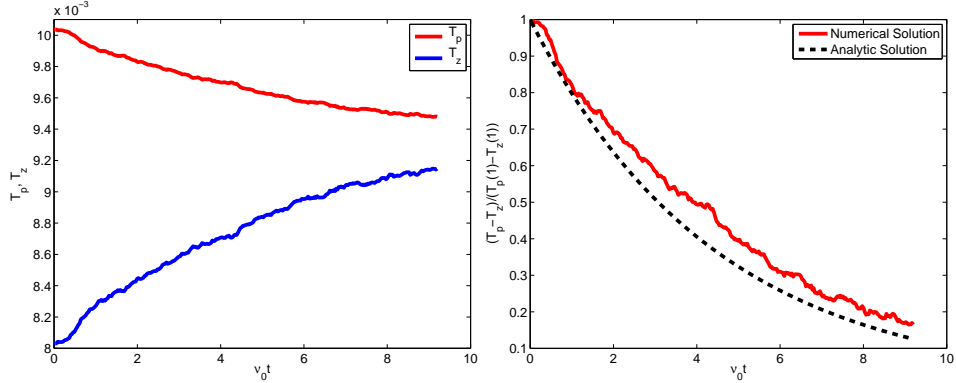
6

Figure 1: Time relaxation of anisotropic temperatures due to collisions

The function $D_{\alpha\beta}$ is defined by an infinite sum of Legendre polynomials, see [6] for details. Within an error of $O(\Delta t)$, $D_{\alpha\beta}$ can be further approximated by functions which are simpler and easier to be computed. In particular, $D_\star$ can be defined as follows:

$$D_\star(\mu, \tau) = \frac{A}{4\pi \sin hA} \exp \mu A.$$

In this case, the distribution of accumulated scattering angle of Nanbu's method is $F(\chi_N) = 2\pi \sin \chi_N D_\star(\cos \frac{\chi_N}{2}, \frac{s}{2})$, and the method may be considered as a special case of a general framework developed in [6]. We note that both TA and Nanbu's methods integrate the Fokker-Planck equation from t to $t + \Delta t$ with an explicit scheme using only velocity distribution function data evaluated at t; such an integration scheme is no better than first-order accurate in Δt. Error accumulation in the TA and Nanbu methods is examined in the convergence analysis in Sec. 4.

III.   TEST CASE AND DEFINITIONS

We perform simulations for the equilibration of a plasma which has a spatially homogeneous distribution function with anisotropic initial temperature for an electron-electron case and for an electron-ion collision case. Due to the stochastic nature of the Monte Carlo model, we extract the deterministic errors by computing the mean of multiple statistically independent solutions. The stochastic errors are computed using the empirical variance of these solutions. The comparison includes both the deterministic errors and stochastic errors when the time steps or number of particles are varied. The error in the numerical solution

is evaluated by comparing it to a highly accurate solution, using a very small time step and a large number of particles.

A. Test Case

Our task is to compare the accuracy of the two collision models. For this reason, we assume spatial homogeneity and that no electrical or magnetic fields exist in the system. Then the physical governing equation becomes the following:

$$\frac{\partial f_\alpha}{\partial t} = \left(\frac{\delta f_\alpha}{\delta t}\right)_c$$

$$f_\alpha(\mathbf{v}, 0) = f_{\alpha 0}(\mathbf{v}).$$

TA and Nanbu's collision methods are numerical approximations to the analytic model of the Fokker Planck collision term $\left(\frac{\delta f_\alpha}{\delta t}\right)_c$.

We consider the time relaxation of charged particles due to electron and electron collisions or electron and ion collisions. The initial distribution has small anisotropy, *i.e.* the parallel temperature and the perpendicular temperature are slightly different, as shown in Figure 1 at $t = 0$. Specifically we use $T_z = 0.008$ and $T_p = 0.01$ for our simulation.

An approximate analytic solution of the test case was derived in [8] using Fokker Planck equation in Landau form and assuming small temperature anisotropy. In [8] the initial distribution is assumed to be the following:

$$f_0(0, \mathbf{v}) = \left(\frac{m}{2\pi}\right)^{3/2} \frac{1}{\sqrt{T_\| T_\perp}} \exp\left(-\frac{mv_\|^2}{2T_\|} - \frac{mv_\perp^2}{2T_\perp}\right).$$

The temperature T of the system is

$$T = \frac{1}{3}T_\| + \frac{2}{3}T_\perp.$$

The conservation of the kinetic energy implies T is constant at all time, hence we have

$$\frac{dT_\perp}{dt} = -\frac{1}{2}\frac{dT_\|}{dt} = \int \frac{df}{dt}\frac{mv_\|^2}{2}d\mathbf{v}$$

Replacing $\frac{df}{dt}$ by the Fokker Planck operator, and assuming $|T_\| - T_\perp| < T_\|$, the following equation was derived:

8

$$\frac{dT_\perp}{dt} = -\frac{1}{2} \cdot \frac{dT_\parallel}{dt} = -\frac{T_\perp - T_\parallel}{\frac{15}{8}\sqrt{2\pi}\tau_0(T)}$$

then

$$\frac{d\Delta T}{dt} = 3 \cdot \frac{dT_\perp}{dt} = -\frac{\Delta T}{\tau}$$

$$\tau = \frac{5}{8}\sqrt{2\pi}\tau_0(T),$$

and

$$\tau_0(T) = \frac{\sqrt{m_\alpha}}{\pi\sqrt{2}e_\alpha^4}\frac{T^{3/2}}{\ln \Lambda n_\alpha}.$$

Then we have

$$\Delta T(t) = \Delta T e^{-\frac{t}{\tau}}.$$

B. Simulations

We perform two types of comparison for the $e-e$ case and for the $e-i$ case. For the first type of comparison, we keep the number of particles N at a constant value in the simulation and compare the numerical results at different time steps Δt. This comparison enables us to see how changes in time step Δt will effect the accuracy of the simulation solutions. In the second comparison, we keep the time step Δt constant and vary the number of particles N in the simulation. This enables us to see how changes in particle number N will effect the accuracy of the simulation solutions. We also perform more than one set of simulations for each type of comparison. For example, we perform simulation on $N = 200$ and 3200, and for each N we perform simulation at various Δt, see figure 2. This way we can see the effects of N on the simulation results over different Δt's.

To separate the effects of stochastic fluctuations from deterministic errors, we compute the mean and variance of M independent solutions. We call the average of such M independent realizations the deterministic solution $\bar{u}$

$$\bar{u}(\Delta t, N) = \frac{1}{M}\sum_{i=1}^{M} u_i$$

where $u_i = u_i(\Delta t, N)$ is the ith independent realization of the solution, and $\bar{u}$ is the average of these independent realizations.
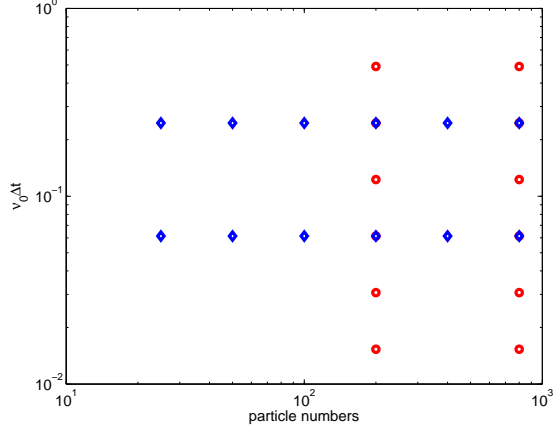
9

Figure 2: $\nu_0 \Delta t$ and N combinations

We designate $e_D(\Delta t, N)$ as the deterministic error when the time step is Δt and the number of particles is N. Specifically, let u_f be a numerical solution computed using a large number of particles and a small time step. An error $e_D(\Delta t, N)$ is defined as the difference between the average of M independent solutions computed using Δt and N and a fine solution u_f. In other words,

$$e_D(\Delta t, N, t) = |\bar{u}(\Delta t, N, t) - u_f(t)|.$$

The quantity $\sigma^2 = \sigma^2(\Delta t, N)$ represents the stochastic fluctuations of the M independent solutions computed at a time step Δt and a number of particles N. σ^2 is defined by the empirical variance in the following way:

$$\sigma^2(\Delta t, N) = \frac{1}{M} \sum_{i=1}^{M} (u_i - \bar{u})^2.$$

Hence $\sigma^2(\Delta t, N)$ represents the mean square deviation of the realizations u_i from the average solution $\bar{u}$.

To compute the order of accuracy with respect to time step Δt, we first compute the error ratio $R(\Delta t)$

$$R(\Delta t) = \left| \frac{\bar{u}(4\Delta t) - \bar{u}(2\Delta t)}{\bar{u}(2\Delta t) - \bar{u}(\Delta t)} \right|.$$

Let u_0 be the exact solution, and assume the average solution $\bar{u}$ has order of accuracy of r, i.e.

$$\bar{u}(\Delta t) = u_0 + C(\Delta t)^r.$$

10

where C is a constant. Then

$$R(\Delta t) = 2^r$$

and therefore the order of accuracy r

$$r = \log_2 R(\Delta t).$$

For all the computations we present here, u_i represents the temperature difference between parallel direction T_z and perpendicular direction T_p normalized by the initial temperature difference. That is

$$u_i(t) = \frac{T_z(t) - T_p(t)}{T_z(0) - T_p(0)}$$

is used in the formulas above to define $\bar{u}$ and u_f. In the computational results described in Sections IV, we have used 160,000 independent simulations. These were divided into $M = 160$ groups of 100 simulations each with N particles. The temperatures T_z and T_p were computed by averaging over each group of 100 simulations. Then the average $\bar{u}$ and the variance σ^2 were computed by averaging over the $M = 160$ groups.

IV.   CONVERGENCE RESULTS

The graphs of the computational results are organized as follows:

The first three plots show the simulation of deterministic solutions when N is constant, and Δt varies:

- The average of 160,000 independent solutions are shown in figure 3 for e-e collisions and in figure 10 for e-i collisions. The independent simulations were used both to compute temperatures and to compute averages, as described at the end of Section III.

- The pointwise errors are shown in figure 4 for e-e collisions and figure 11 for e-i collisions.

- The pointwise order of accuarcy $r = \log_2 R(\Delta t)$ are shown in figure 5 for e-e collisions.

The next two plots show the deterministic solutions when Δt is constant, and N varies:

- The average of 160,000 independent solutions are shown in figure 6 for e-e collisions and figure 12 for e-i collisions.

11

- The deterministic pointwise errors e_D are shown in figure 7 for e-e collisions and figure 13 for e-i collisions.

The simulation of stochastic fluctuations is shown in the following part of the graphs:

- Figure 8 and figure 14 show the stochastic fluctuations when N is constant and Δt varies for e-e collisions and e-i collisions, respectively .

- Figure 9 and figure 15 show the stochastic fluctuations when Δt is constant and N varies for e-e collisions and e-i collisions, respectively.

The convergence results are presented in the following manner. We first present results computed using Nanbu's method and then results computed using TA's method. In the discussion about each method, we first describe the results of deterministic (*i.e.* averaged) solutions. We show the simulations with constant number of particles N and varying time step Δt, as well as constant Δt and varying N. In order to understand the order of time step accuracy, we also include the pointwise error ratio r. We then explain the results of stochastic fluctuations with the same set of Δt and N combinations as the deterministic case.

For all the plots presented here, computational results obtained using Nanbu's method are shown in the left-hand column, whereas results obtained using TA's method are represented in the right-hand column.

The fine solution u_f we use in the convergence results is obtained using 6,400 particles and $v_0 \Delta t = 0.0076$.

A. Simulation Results Using Nanbu's Method

In this section, we present the simulation results using Nanbu's model. We discuss both the e-e and the e-i cases.

1. *Deterministic Solutions $\bar{u}(\Delta t, N, t)$ and Errors $e_D(\Delta t, N)$*

We begin with the deterministic solutions $\bar{u}$, when N is held constant and equal to 200 and 3200 and Δt varies, see figure 3 for the e-e case and figure 10 for the e-i case. It is evident that

random fluctuations from the Monte Carlo simulation are eliminated after computing the average solutions, resulting in smooth time relaxation curves $\bar{u}$. Clearly, when the time step Δt is smaller, simulation solutions approach the fine solution u_f. Additionally, if the number of particles is increased, we also see an improvement in accuracy. Figure 4 (e-e) and figure 11 (e-i) shows the result that when we keep N constant, $e_D(\cdot, N)$ decreases as Δt becomes smaller. To see the order of accuracy, we compute the order of accuracy $r = \log_2 R(\Delta t)$. In the e-e case, Nanbu's method does not produce a precise order of accuracy but rather oscillates around the value $r = 0.5$, see figure 5. In the e-i case, we could not reach a conclusion about the order of accuracy so the corresponding figure is not included.

When Δt is held constant and N increases, the results for the e-e and the e-i cases are relatively different. In the e-e case, the average solutions approach the fine solution u_f , see figure 6. The corresponding pointwise errors $e_D(\Delta t, \cdot)$ of the average solutions $\bar{u}$ are depicted in figure 7. For each constant time step Δt, $e_D(\Delta t, \cdot)$ decreases linearly as the number of particles N increases. In other words, the order of accuracy for the number of particles is $O(N^{-1})$. Moreover, as might be expected, for any number of particles N, $e_D(N, \Delta t = 0.0613)$ is less than $e_D(N, \Delta t = 0.24525)$. In the e-i case, we see generally the errors $e_D(\Delta t, N)$ decrease when the number of particles N increases, but the result is not as clearcut as the e-e case, see figure 12 and figure 13.

2. Stochastic Fluctuations $\sigma^2(\Delta t, N)$

The numerical solutions computed using the Monte Carlo method are composed of deterministic components and stochastic fluctuations. In order to completely understand the statistical accuracy of the solutions, we analyze the stochastic fluctuations σ^2 of the solutions.

We first calculated the stochastic fluctuations $\sigma^2(\cdot, N)$ at various time steps Δt for $N = 200$ and 3200 and $16,000$ realizations. From figure 8 (e-e case) and figure 14 (e-i case) we can see that for each constant N, stochastic fluctuations $\sigma^2(\cdot, N)$ have approximately the same values and are independent of the time steps Δt's. In other words, reducing the time step Δt does not have any influence on $\sigma^2(\cdot, N)$.

We then compute $\sigma^2(\Delta t, \cdot)$ when the time step Δt is held constant. The time step Δt in the e-e case is equal to 0.2452 and 0.06013, and Δt in the e-i case is 0.22214 and 0.05528, see

figure 9 (e-e case) and figure 15 (e-i case). The stochastic fluctuations $\sigma^2(\Delta t, \cdot)$ decreases linearly as the number of particles N increases. This means that the order of particle number accuracy is $O(N^{-\frac{1}{2}})$, and one can reduce random fluctuations by increasing the number of particles N, as is commonly expected.

B. Simulation Results Using TA's Method

In this section, we describe the computational results obtained using TA's method. We perform exactly the same computations as for Nanbu's model. This requires determining the average solutions $\bar{u}$ and errors e_D and stochastic fluctuation σ^2 at various time steps Δt and number of particles N.

1. Deterministic Solutions $\bar{u}(\Delta t, N, t)$ and Errors $e_D(\Delta t, N)$

We use the same procedure as we used with Nanbu's method. Specifically, we compute the average of 16,000 independent solutions when the number of particles N are held constant and equal to 200 and 3200, see figure 3 for the e-e case and 10 for the e-i case. The average solutions eliminate random fluctuations from the Monte Carlo simulation, resulting in smooth time relaxation curves $\bar{u}$. When time step Δt is smaller, simulation solutions approach the fine solution u_f. If the number of particles is increased, we also see an improvement in accuracy. Figure 4 (e-e case) and figure 11 (e-i case) shows that when we keep N constant, $e_D(\cdot, N)$ decreases as Δt becomes smaller.

When Δt is held constant, $\bar{u}$ approaches the fine solution u_f as N increases, as shown in figure 6 (e-e case) and 12 (e-i case), however, the results for e-e and e-i cases are again different. In the e-e case, the corresponding pointwise errors $e_D(\Delta t, \cdot)$ decreases linearly as the number of particles N increases, see figure 7. For any number of particles N, $e_D(N, \Delta t = 0.0613)$ is smaller than $e_D(N, \Delta t = 0.24525)$. In the e-i case, overall the errors $e_D(\Delta t, N)$ decrease when the number of particles N increases, and $e_D(N, \Delta t = 0.0613)$ is generally smaller than $e_D(N, \Delta t = 0.24525)$, but the result is not as distinct as the e-e case, see figure 13.

TA's method in the e-e case yields a clear value of order $r = 0.5$ when the number of particles $N = 3200$, as shown in figure 5; however, we can not obtain the order of accuracy

r through error ratio in the e-i case so that this value is not plotted (as mentioned above).

In general Δt has to be small enough to see any improvement in accuracy when the number of particles N increases. If Δt is too large, the time step errors dominate, and no improvement of accuracy will occur when N increases. Figure 7 also shows the relation between time step errors and particle number errors for the e-e case. When $\Delta t = 0.24525$, we can not reduce the errors e_D by increasing the number of particles N. For the e-i case, the corresponding results are not so clear, so that this figure is omitted.

<center>2.   *Stochastic Fluctuations $\sigma^2(\Delta t, N)$*</center>

The numerical solutions computed using the Monte Carlo method have deterministic components and stochastic fluctuations. We examine the stochastic fluctuations σ^2 of the solutions in this section. We again calculate the stochastic fluctuations $\sigma^2(\cdot, N)$ at various time steps Δt for $N = 200$ and 3200. The e-e case and the e-i case produce similar results. We observe that for each constant N, stochastic fluctuations $\sigma^2(\cdot, N)$ have approximately the same values and are independent of the time steps Δt's, as shown in figure 8 and figure 14. Evidently, reducing the time step Δt does not have significant effect on $\sigma^2(\cdot, N)$. The fluctuations are independent of the time step Δt.

Once again we compute $\sigma^2(\Delta t, \cdot)$ when the time step Δt is kept fixed and is equal to 0.2452 and 0.06013, see figure 9 and figure 15. The stochastic fluctuations $\sigma^2(\Delta t, \cdot)$ diminish linearly as the number of particles N grows. This means when the time step Δt is constant, the fluctuations decrease like $O(N^{-\frac{1}{2}})$.

<center>**C.   Comparison of the two methods**</center>

Simulation results obtained using the TA's model were actually very similar to Nanbu's model in the e-e case and e-i case. Both methods yield a more conclusive results in the e-e case than the e-i case. The major advantage of Nanbu's method is that the results are more accurate in terms of deterministic errors e_D. Specifically, it yields approximately half the pointwise errors $e_D(\Delta t, N)$ compared to TA's method, see figure 4

$$e_{DNanbu}(\Delta t, N) \approx \frac{1}{2} e_{DTA}(\Delta t, N)$$

<center>15</center>

However, as discussed in previous sections of this article, Nanbu's method does not yield a higher order of accuracy r. Using TA's method we obtain a clearly defined r equal to 0.5, whereas the order of accuracy r for Nanbu's method oscillates around 0.5 in the e-e case, as shown in figure 5.

The stochastic fluctuations σ^2 for both methods decreases linearly as N increases, as shown in figure 9:

$$\sigma^2_{Nanbu}(\Delta t, \cdot) \approx c_{Nanbu}(N^{-1})$$

$$\sigma^2_{TA}(\Delta t, \cdot) \approx c_{TA}(N^{-1})$$

where $c_{Nanbu} \approx c_{TA}$ and both are independent of N. However, when the particle number N is held constant, the statistical fluctuations are independent of the time step Δt, and using both methods results in approximately the same fluctuations, see figure 8:

$$\sigma^2_{Nanbu}(\cdot, N) \approx c_{Nanbu}$$

$$\sigma^2_{TA}(\cdot, N) \approx c_{TA}$$

where $c_{Nanbu} \approx c_{TA}$ and both are independent of Δt. As we have pointed out, two error sources, from time step and number of particles, exist in the simulation. One can see the relation between time step errors and particle number errors for both methods from figure 7. To see any improvement in accuracy when the number of particles N increases, Δt has to be small enough so the major errors come from the number of particles N. From this point of view, Nanbu's method also has advantages over TA's method. One can use larger Δt, *i.e.* $\Delta t = 0.24525$, and still see the improvement in accuracy when N increases. This also shows Nanbu's method produces smaller time step errors.

V. SUMMARY AND DISCUSSION

In this paper, we have performed a convergence analysis to compare the two widely-used Monte Carlo binary collision models proposed by Takizuka & Abe and Nanbu. Our test case is a spatially homogeneous plasma with no electric or magnetic fields. We compute the relaxation of anisotropic temperatures over time due to collisions, using the results to evaluate the accuracy and efficiency of these two methods. Extensive simulation results are presented for both electron-electron and electron-ion collision cases. To facilitate the error

analysis, we extract the deterministic errors by computing the mean of multiple statistically independent solutions. The stochastic errors are computed using the empirical variance of these solutions. The comparison includes both the deterministic errors and stochastic errors when the time step or number of particles is varied. We also compute the order of accuracy in time using an error ratio.

There are a number of similarities between the two methods. Both methods yield more conclusive results in the e-e case. In the e-e case, the two methods have the approximately $O(\sqrt{\Delta t})$ time step accuracy computed from log of the error ratio $\log_2 R$. Our convergence results differ from the result described by Bobylev and Nanbu in [6]. According to their derivation of time-explicit formula, the order of time step error is formally $O(\Delta t)$, but our study found the accumulated error scales as $O(\sqrt{\Delta t})$. We do not have a definite explanation for this. One possible reason is that there are only limited number of particles in our simulation, and perhaps our results are still dominated by the errors generated by the particles. Bobylev and Nanbu's time evolution formula does not take into account the finite number of particles, *i.e.,* only time-discretization effects are captured in their formula.

In the e-e case and e-i case, the stochastic fluctuations $\sigma^2(\cdot, N)$ are independent of time step Δt when N is kept fixed, *i.e.*

$$\sigma^2(\cdot, N) \approx c$$

in which c is a constant independent of Δt and is the same for both methods. When Δt is held constant, the fluctuations $\sigma^2(\Delta t, \cdot)$ diminish linearly when the number of particles N grows, *i.e.*

$$\sigma^2(\Delta t, \cdot) \approx cN^{-1}$$

in which c is a constant independent of N and is the same for both method In our analysis, the overall errors come from two sources: deterministic errors due to the time step and random errors due to the number of particles. Another similarity between the two methods is that the errors originating from one source - either time step Δt or number of particles N- may dominate the total errors. For example, to see the decrease in errors when Δt decreases, N has to be large enough and Δt cannot be too small. Once Δt becomes too small, we cannot see any improvement in accuracy when reducing the time step Δt unless we increase the number of particles N.

While both methods have the same order of accuracy $O(\sqrt{\Delta t})$ in the e-e case, Nanbu's method is more accurate. Specifically, it produces time step error that is smaller by a factor of $1/2$, *i.e.* :

$$e_{DNanbu}(\Delta t, N) \approx \frac{1}{2} e_{DTA}(\Delta t, N)$$

This means that Nanbu's method can use $4\Delta t$ to achieve the same accurate results as TA's method. This translates to a considerable savings in time and cost.

Nanbu's method is more complicated and therefore harder to implement. Nanbu's method involves solving a nonlinear function for A for every s. However, the value of A can be computed in advance and stored in a table; therefore, this disadvantage is not that significant because ultimately it does not slow down the computation.

To conclude, many similarities exist between the two methods. However, we note the advantage of Nanbu's method in reducing the computational cost and achieving higher accuracy. We are currently exploiting Nanbu's method in extending the earlier hybrid method developed for rarefied gas to the simulation of plasmas with Coulomb collisions with improved computational efficiency.

VI.   ACKNOWLEDGMENTS

[1] O.V. Batishchev, M. M. Shoucri, A. A. Batishcheva and I. P. Shkarofsky. J. Plasma Physics, Vol 61, part 2, p. 347-364 (1999).

[2] L. Spitzer, Jr., Physics of Fully Ionized Gases, 2nd ed. (Interscience, New York, 1967).

[3] T. Takizuka and H. Abe, J. Comp. Phys. 25 (1977).

[4] K. Nanbu, Phys. Rev. E. 55 (1997).

[5] R. E. Caflisch and L. Pareschi. J. Compt. Phys. 154, 96 (1999).
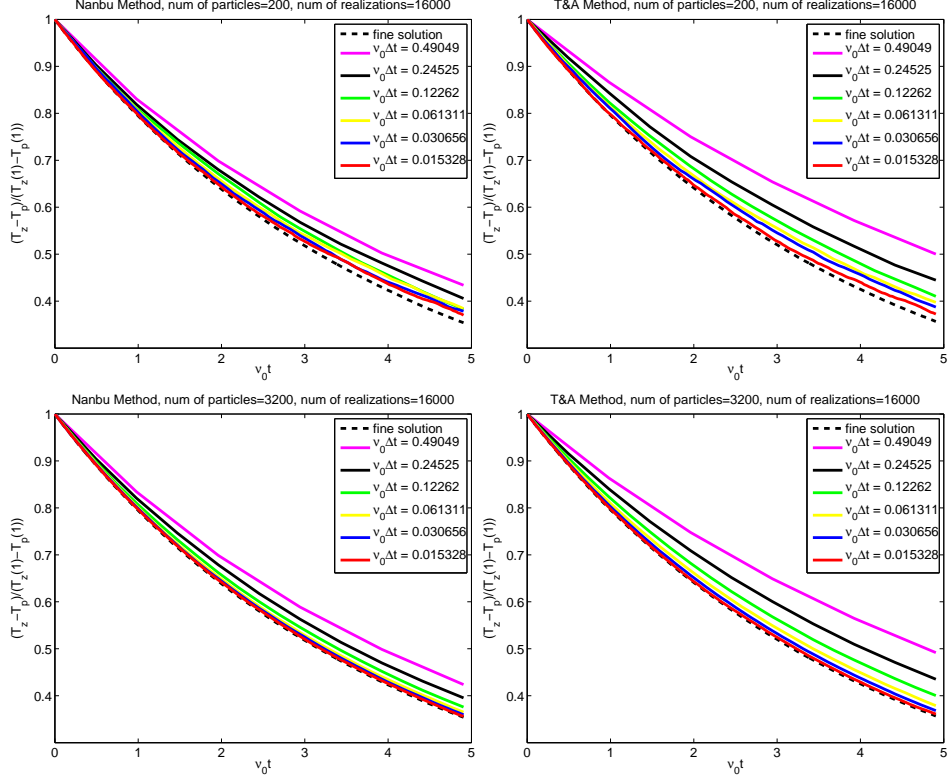
Figure 3: (e-e case) Average solutions $\bar{u}(\cdot, N)$; The results using Nanbu's method are depicted in the left-hand column; results using TA's method are shown in the right-hand column. In each graph, the top row results are computed using $N = 200$ particles and the bottom row results use $N = 3200$; average of 16,000 independent realizations.

[6] A. V. Bobylev and K. Nanbu, Physical Review E, Vol 61, No. 4, p. 4576-4582 (2000).

[7] M. N. Rosenbluth, W. M. MacDonald, and D. L. Judd, Phys. Rev. 107, 1 (1957).

[8] B. A. Trubnikov, Review of Plasma Physics (Consultant Bureau, New York, 1965), Vol. 1, p. 105.
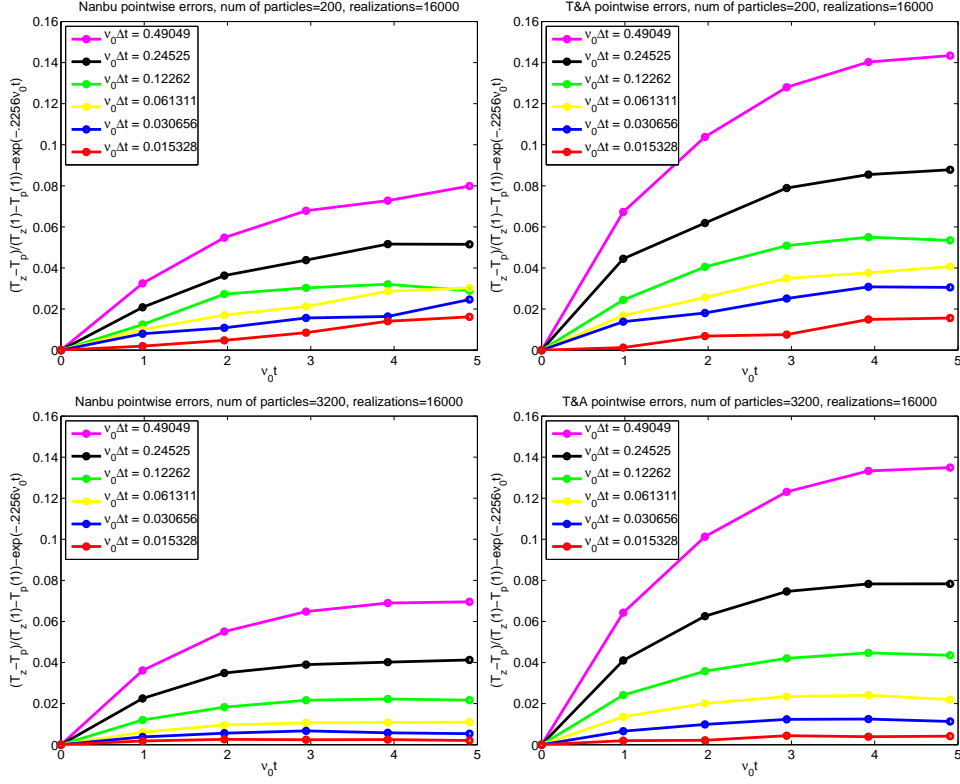
Figure 4: (e-e case) Deterministic errors e_D; the results using Nanbu's method are depicted in the left-hand column; results using TA's method are shown in the right-hand column. In each graph, the top row results are computed using $N = 200$ particles and the bottom row results using $N = 3200$; average of 16,000 independent realizations.
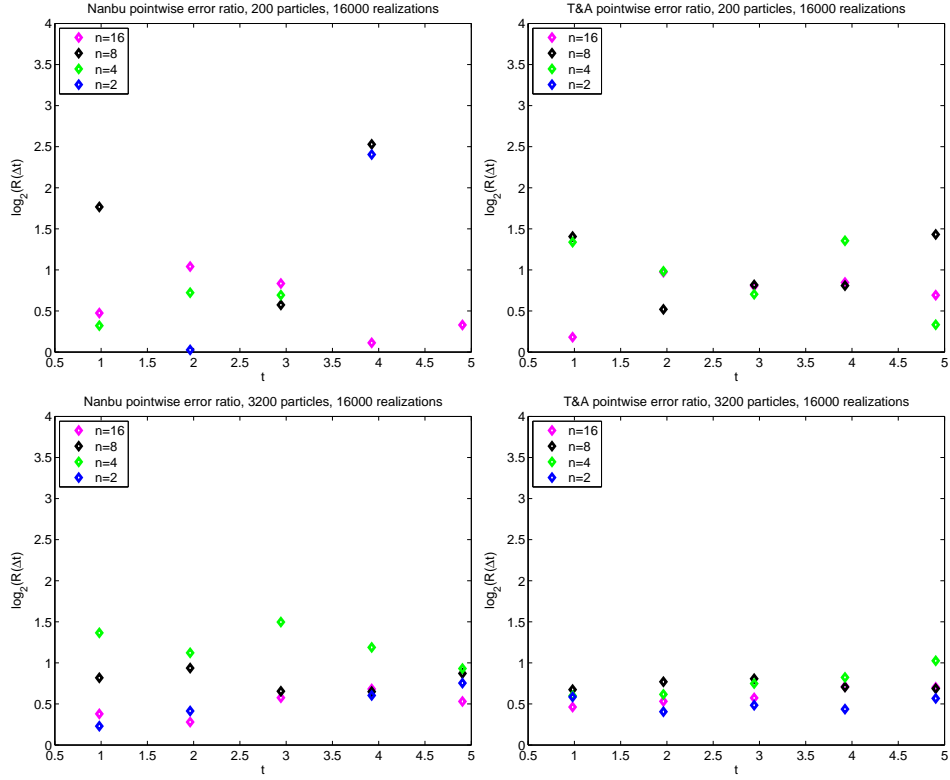
Figure 5: (e-e case) Order of accuracy $r = \log_2 R(\Delta t)$; the results using Nanbu's method are depicted in the left-hand column; results using TA's method are shown in the right-hand column. In each graph, the top row results are computed using $N = 200$ particles and the bottom row results using $N=3200$; average of 16,000 independent realizations.
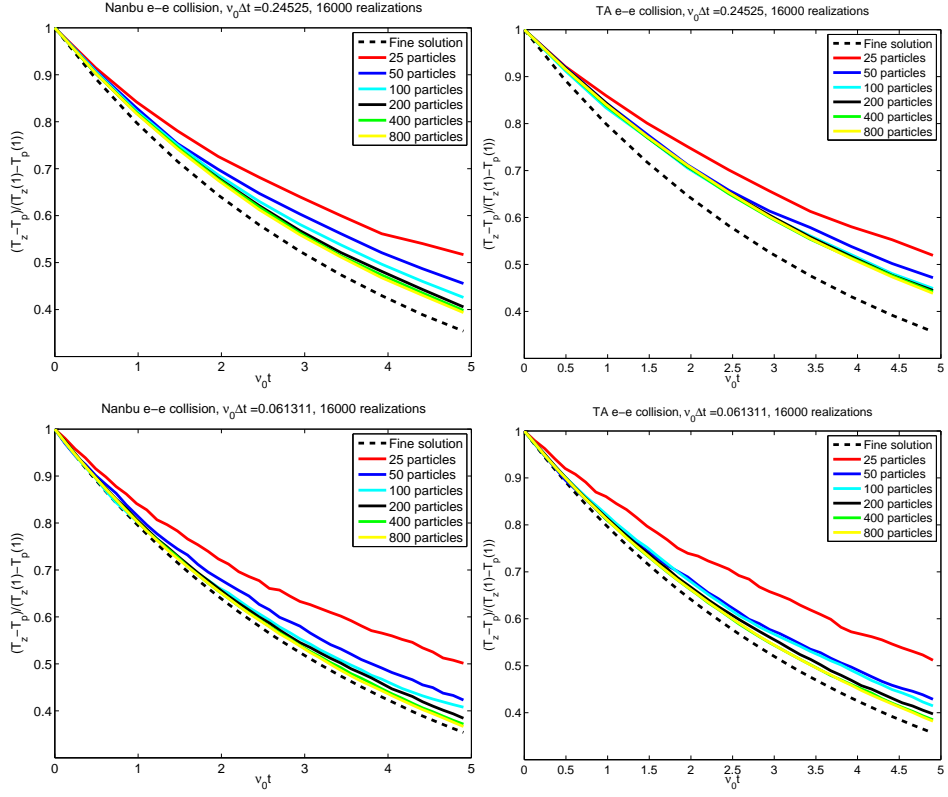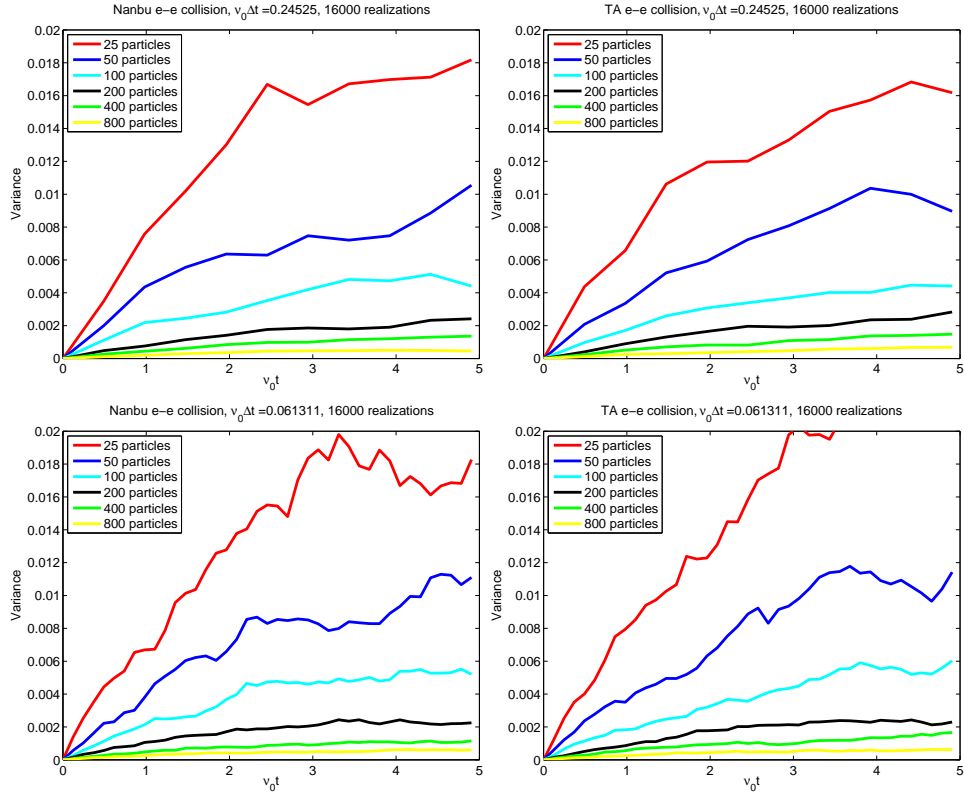
Figure 6: (e-e case) average solutions; the results using Nanbu's method are depicted in the left-hand column; results using TA's method are shown in the right-hand column. In each graph, the top row results are computed using $\nu_0\Delta t = 0.24525$, and the bottom row results using $\nu_0\Delta t = 0.0613$.
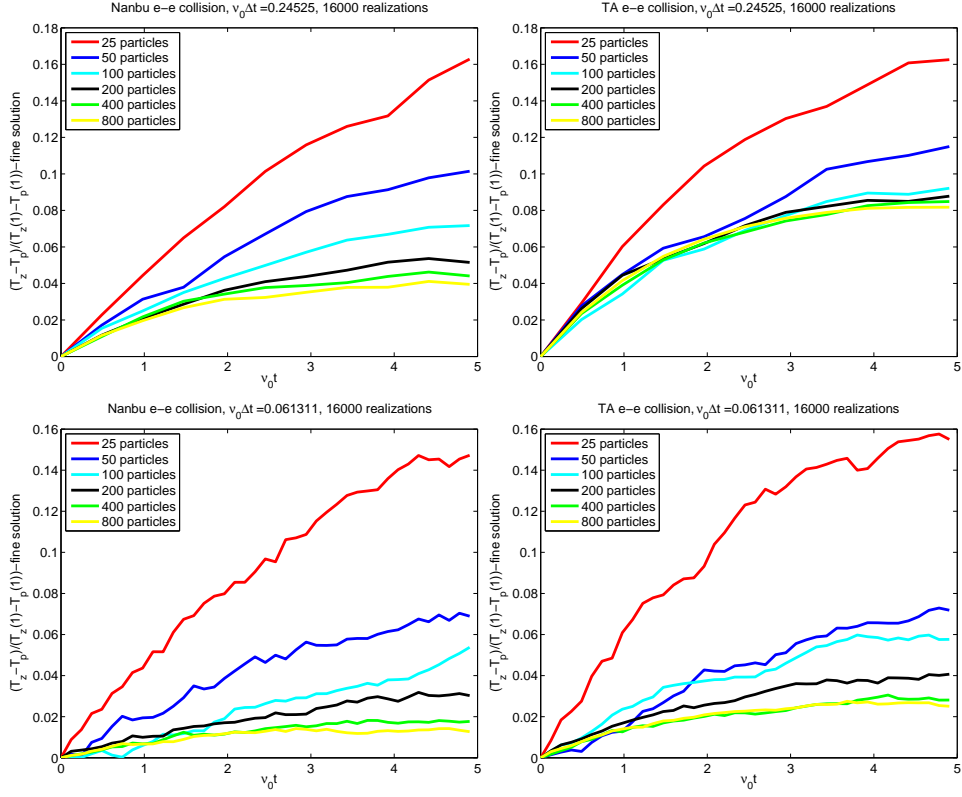
Figure 7: (e-e case) Deterministic error; The results using Nanbu's method are depicted in the left-hand column; results using TA's method are shown in the right-hand column. In each graph, the top row results are computed using $\nu_0 \Delta t = 0.24525$, and the bottom row results using $\nu_0 \Delta t = 0.0613$
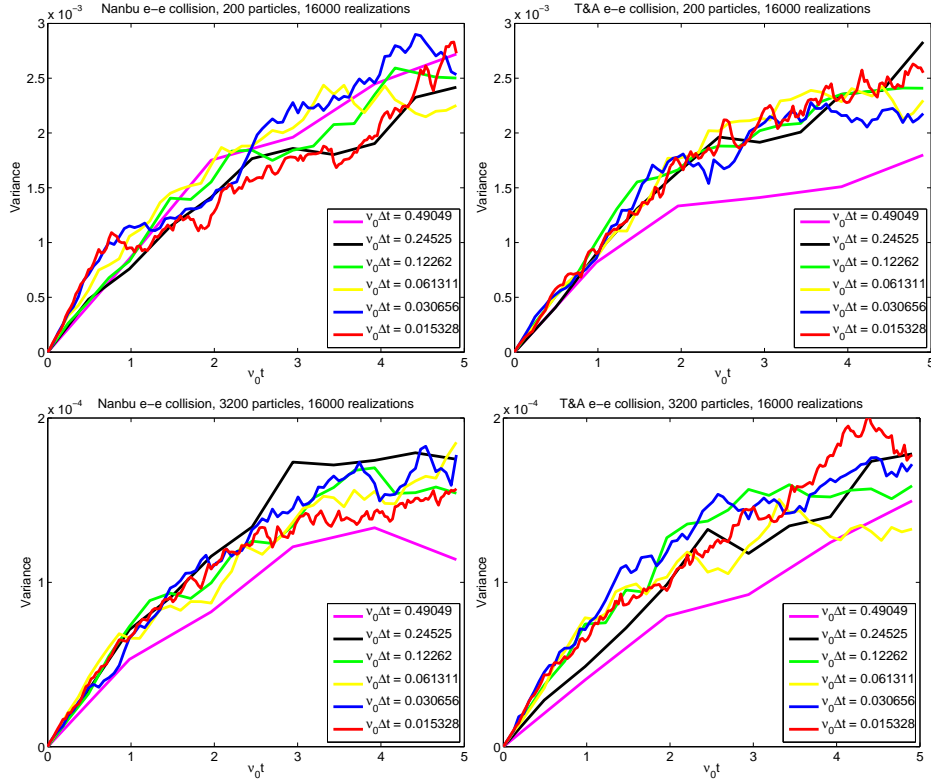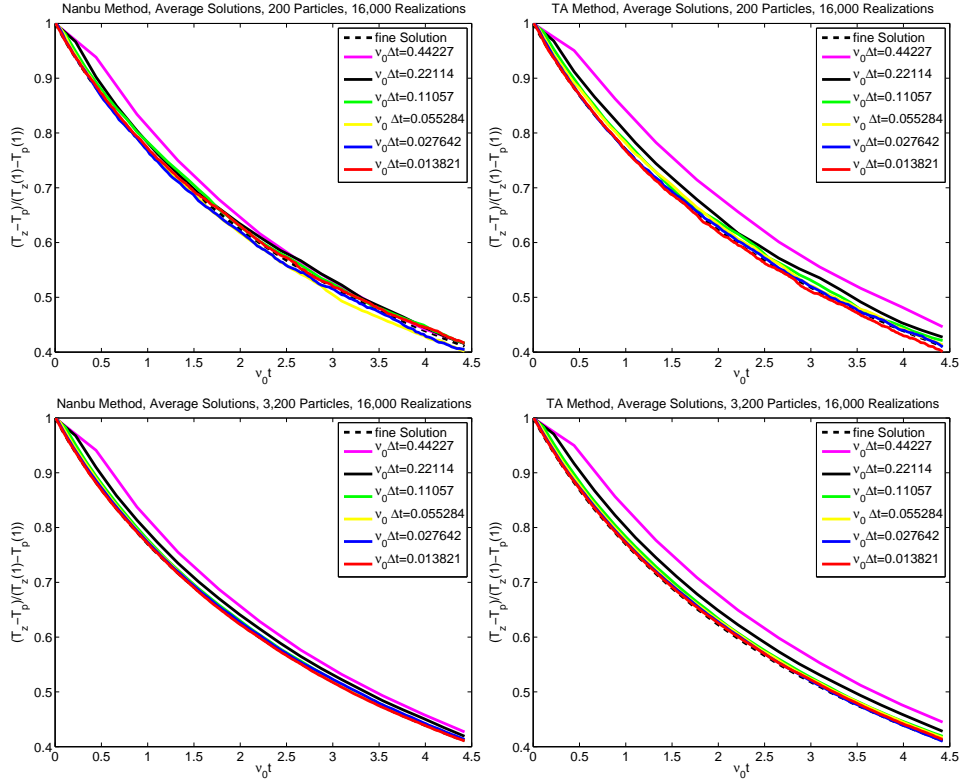
Figure 8: (e-e case) Variance σ^2 of the results using Nanbu's method are depicted in the left-hand column; results using TA's method are shown in the right-hand column. In each graph, the top row results are computed using $N = 200$ particles and the bottom row results using $N=3200$; average of 16000 independent realizations.
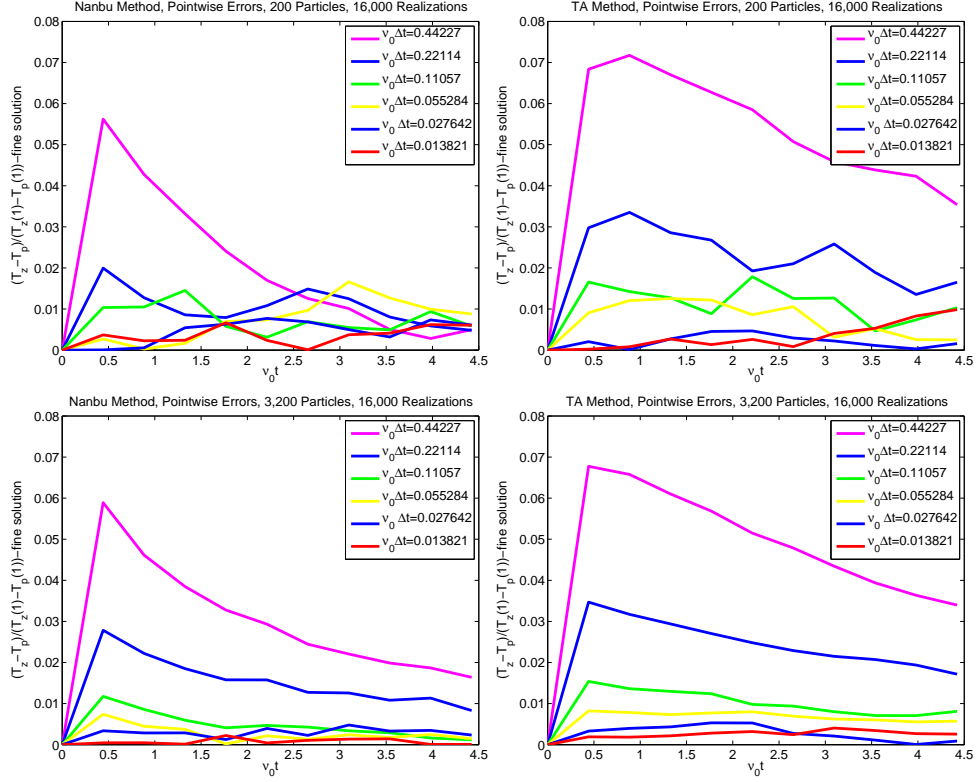
Figure 9: (e-e case) Variance σ^2 of the results using Nanbu's method are depicted in the left-hand column; results using TA's method are shown in the right-hand column. In each graph, the top row results are computed using $\nu_0 \Delta t = 0.24525$, and the bottom row results using $\nu_0 \Delta t = 0.0613$.

Figure 10: (e-i case) Average solutions $\bar{u}(\cdot, N)$; The results using Nanbu's method are depicted in the left-hand column; results using TA's method are shown in the right-hand column. In each graph, the top row results are computed $N = 200$ particles and the bottom row results using $N{=}3200$; average of 16,000 independent realizations.
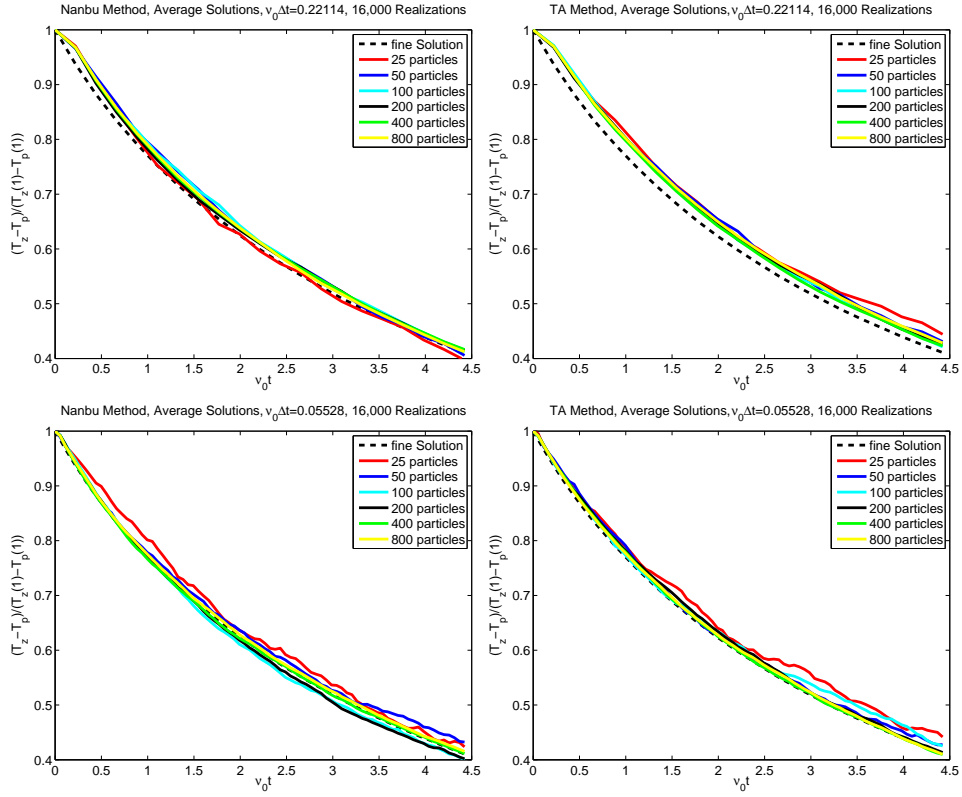
Figure 11: (e-i case) Deterministic errors e_D; the results using Nanbu's method are depicted in the left-hand column; results using TA's method are shown in the right-hand column. In each graph, the top row results are computed using $N = 200$ particles and the bottom row results using $N=3200$; average of 16000 independent realizations.

Figure 12: (e-i case) average solutions; The results using Nanbu's method are depicted in the left-hand column; results using TA's method are shown in the right-hand column. In each graph, the top row results are computed using $\nu_0 \Delta t = 0.2211$, and the bottom row results using $\nu_0 \Delta t = 0.05528$.
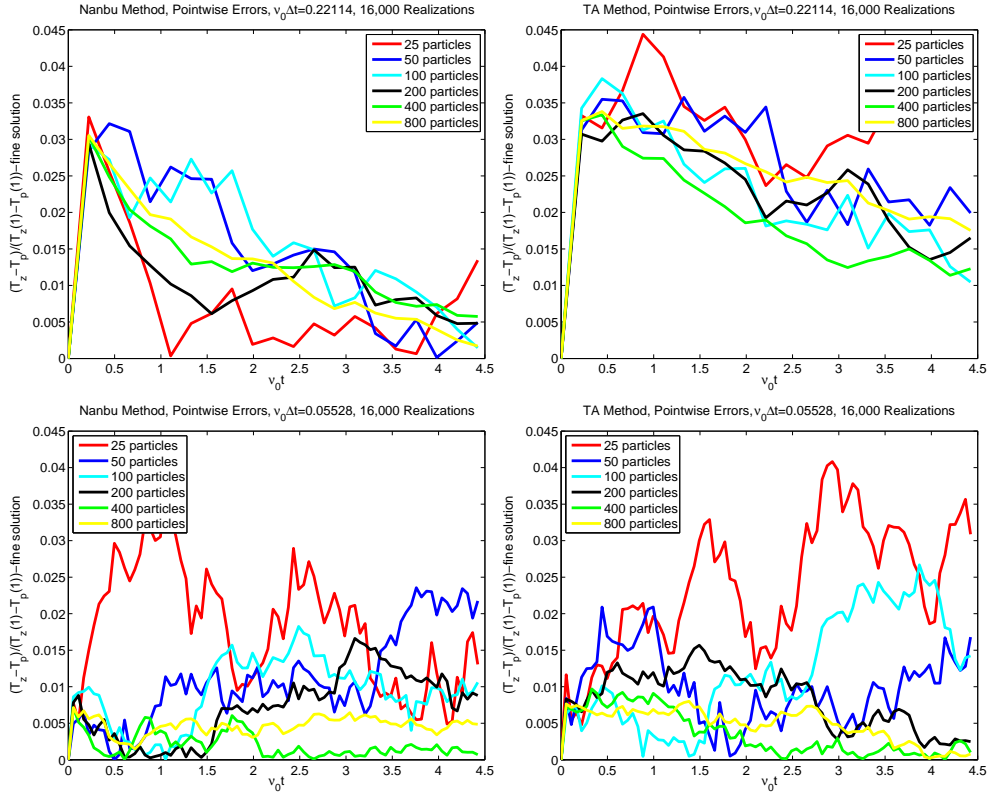
Figure 13: (e-i case) Deterministic error; the results using Nanbu's method are depicted in the left-hand column; results using TA's method are shown in the right-hand column. In each graph, the top row results are computed using $\nu_0\Delta t = 0.2211$, and the bottom row results using $\nu_0\Delta t = 0.05528$.
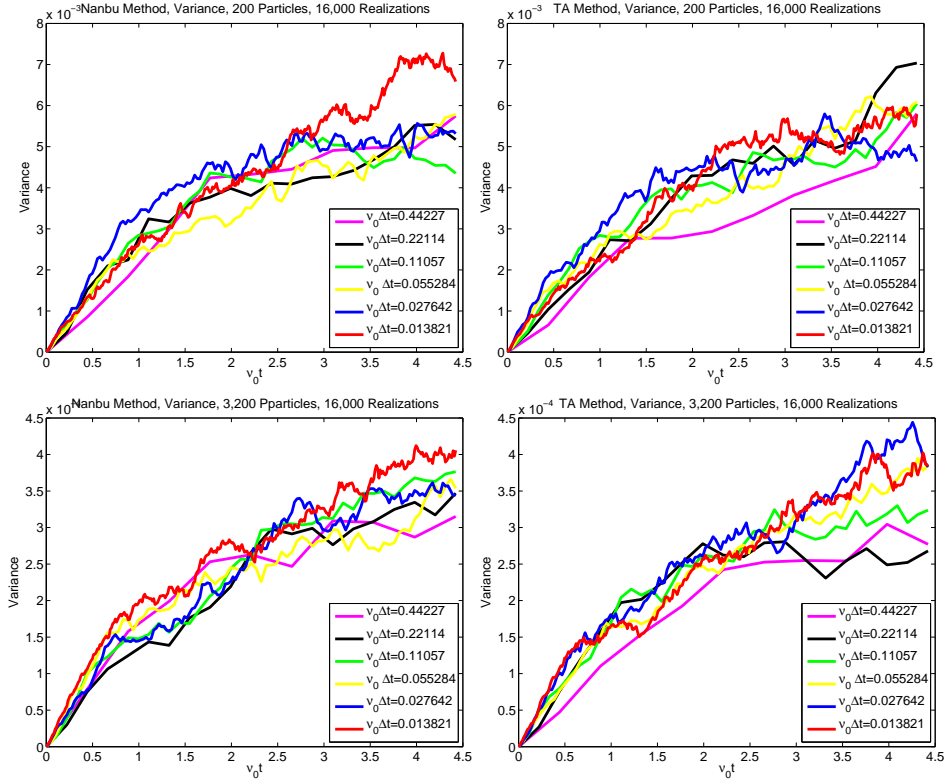
Figure 14: (e-i case) Variance σ^2 of the results using Nanbu's method are depicted in the left-hand column; results using TA's method are shown in the right-hand column. In each graph, the top row results are computed using $N = 200$ particles and the bottom row results using $N=3200$; average of 16,000 independent realizations.
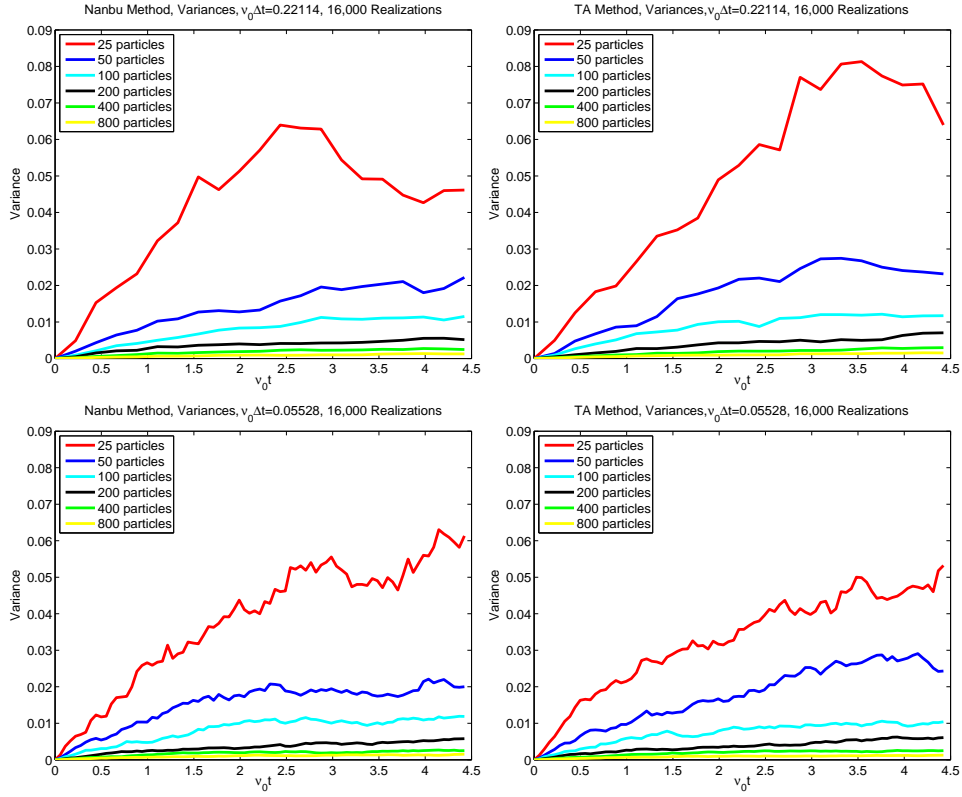
Figure 15: (e-i case) Variance σ^2 of the results using Nanbu's method are depicted in the left-hand column; results using TA's method are shown in the right-hand column. In each graph, the top row results are computed using $\nu_0 \Delta t = 0.2211$, and the bottom row results using $\nu_0 \Delta t = 0.05528$.